*Journal of Sound and Vibration* (1981) **79**(1), 61–77

# A THEORETICAL STUDY OF LIMIT CYCLE OSCILLATIONS OF PLENUM AIR CUSHIONS

M. J. HINCHEY AND P. A. SULLIVAN

*Institute for Aerospace Studies, University of Toronto, Toronto, Canada*

(*Received* 15 *November* 1978, *and in revised form* 1 *May* 1981)

Air cushion vehicles (ACV) are prone to the occurrence of dynamic instabilities which frequently appear as stable finite amplitude oscillations. The aim of this work is to ascertain if the non-linearities characteristic of ACV dynamics generate limit cycle oscillations for cushion systems operating at conditions for which a linear theory predicts instability. The types of non-linearity that can occur are discussed, and an analysis is presented for a single cell flexible skirted plenum chamber constrained to move in pure heave only. Two cushion feed cases are considered: a plenum box supply and a duct. The results obtained by a Galerkin/describing function analysis are compared with those generated by a full numerical simulation. For the plenum box supply system, it is shown that the limit cycles can be suppressed by using a piston to introduce high frequency small amplitude volume oscillations into the plenum chamber.

## 1. INTRODUCTION

A problem that has been encountered during the development of various types of air cushion vehicle (ACV) is the sporadic occurrence of self-excited oscillations. Frequently these oscillations are simply a translation in the vertical direction, that is, a pure heave, but other motions have been observed. For some applications, they may only be of nuisance value, and a nominal change in operating conditions is often sufficient to suppress them. However, they can cause operational difficulties [1] and, in extreme cases, lead to destruction of the vehicle. Furthermore, the limited amount of evidence available from industrial practice indicates that their onset may be governed by many factors, two recently documented examples of which are (i) the cushion as a wave generator or pump when hovering over water at zero forward speed [2], and (ii) the inherent non-linear characteristics of the material used in the flexible inflated structure or "skirt" characteristic of the modern ACV [2, 3].

Significant progress in understanding ACV dynamics has been made by many authors using linear analysis techniques. Prominent among these are the contributions made by Richardson and others at the Massachusetts Institute of Technology [4, 5]. They pointed out that, for a cushion operating at low pressure, although the air escape process can be assumed to be incompressible, the air in the cushion volume has to be considered compressible. For a linear analysis, the cushion volumes are therefore modelled as lumped pneumatic capacitances. Hinchey and Sullivan [6] analyzed the structure of stability boundaries for a family of duct supply systems in terms of the two parameters of basic design interest: cushion pressure and cushion volume flow. This analysis indicated that even relatively short ducts could have a major destabilizing effect, and that the primary source of the effect was the inertia of the air in the duct. More recently, Hinchey [7] has shown that, under suitably controlled experimental conditions, these boundaries can be accurately reproduced. These and other experiments [5] therefore generally confirm



0022-460X/81/210061+17 $02.00/0 

the validity of the assumptions used in the linear analytical models of cushion dynamics described above.

Very little work on non-linear ACV dynamics is available in the open literature. However, non-linear effects may have practical significance. For example, Leatherwood [8], using an analog computer simulation, showed that small transient disturbances superimposed on a sinusoidal input could generate large subharmonic responses. Also, non-linear stability problems can occur in practice. Such instabilities have been observed for two radically different cushion geometries constrained to move in two degrees of freedom: that is, heave and a rotation which is equivalent to pitch or roll; these systems were found to be stable for small initial pitch angles but clearly unstable beyond a certain critical angle [3].

A fundamental limitation of a linear analysis is that, although it may predict a divergent oscillation at the onset of instability, it cannot predict the ultimate nature of the motion. Observations of laboratory experiments and numerical simulations [6, 7] suggest that the motion is frequently a stable finite amplitude oscillation which is a limit cycle, since the fluid flow processes involve turbulent and viscous decay phenomena [9]. The purpose of the work reported in what follows here is to ascertain if the non-linearities that are characteristic of air cushion dynamics can cause such oscillations near linear stability boundaries. Only a very simple case is considered; this is a single cell flexible skirted plenum chamber constrained to move in pure heave. The cushion air supply system is modelled in two ways: as a plenum box and as a duct. The basic geometries are shown in Figure 1.

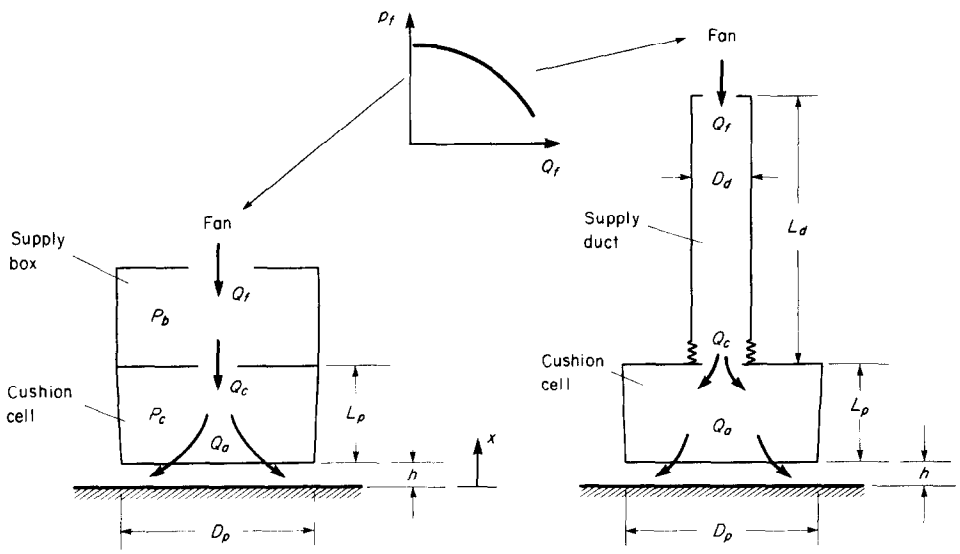


Figure 1. Basic air cushion geometries studied.

## 2. NON-LINEARITIES IN AIR CUSHION DYNAMICS

The mathematical models of cushion dynamics described in references [4–7] include several non-linear features. The source of cushion air—usually a fan or blower—often has a non-linear static pressure–volume flow relationship or "characteristic". For sufficiently high cushion oscillation frequencies or for very low cushion flow rates the aerodynamics of unsteady flow through the fan blades will be significant, and at sufficiently large amplitudes, non-linear effects will be present. The compression expansion process

in the cushion volume itself is usually modelled by a polytropic equation of state $P_c/\rho^n = \text{constant}$, where $P_c$ is the absolute cushion pressure, $\rho$ is the cushion air density, and $n$ is assumed to be equal to the specific heat ratio, $= \gamma = C_p/C_v$ [3, 4]. This may contribute significant non-linear effects if the amplitude of the pressure oscillations is large compared with the atmospheric pressure.

The unsteady air escape process from the cushion to the atmosphere is usually assumed to be quasi-steady, and is consequently modelled by the one-dimensional orifice flow law based on Bernoulli's law and a suitable discharge coefficient [3, 4]. The frequency of oscillation is usually low enough to make this approximation acceptable [6], but it has two associated non-linearities. One is the square-root dependence of the volume flux of air on the cushion pressure coupled to the varying cushion air escape area. In the simplified model of Figure 1, this area is directly proportional to the hovergap $h$. The second is characteristic of vehicles equipped with flexible skirts. For sufficiently large amplitude oscillations, skirt–ground contact occurs, and there is an abrupt change in the functional relationship between the air escape area and vehicle heave height. In the case depicted in Figure 1, as soon as skirt–ground contact occurs, the cushion air flow is, for all practical purposes, completely shut off [10]. For more complex skirt geometries and for hover over irregular surfaces, the transition to shut-off is not so abrupt, but it is clear that this "valving"—as it has been called [1]—can have a major effect on the system dynamics. The amplitudes of the oscillations are usually large enough to cause valving.

Finally, it is now known that under certain circumstances the static heave, pitch and roll stiffness characteristics of flexible skirted cushions can display significant hysteretic behaviour. This on its own can cause a system to enter a limit cycle [9, p. 196]. At least three possible sources have been identified [3, 10, 11]. One is a structural instability: that is, flexible skirts are pressure-stabilized membrane structures, and for certain skirt geometries and under certain load conditions they can buckle in such a way as to cause loss of the cushion seal; this in turn causes cushion venting and large reductions in cushion pressure. A second possible source is sliding friction forces generated by those parts of the skirt which are in contact with the ground and which move relative to it when the vehicle moves [3]. A third is related to the ability of the skirt system to transmit the small forces generated during the loading portion of a skirt contact cycle where the skirt is pushed down on to the ground [10]. These forces are not present during the unload portion owing, apparently, to stress relaxation phenomena characteristic of certain elastomers. Although all three phenomena have been observed during laboratory model tests, their practical significance remains to be determined. For example, the first mechanism has been observed at full scale [1], but only for particular geometries [10, 11]. Sullivan *et al.* have been able to demonstrate that the second does not occur for some skirt systems but may be significant for others [3, 10, 11]. The third can have very large effects on vehicle dynamics at model scale [3], but it occurs only for certain types of skirt material, and it is currently not clear if it is significant at full scale or on adequately modelled skirts.

Not all of these non-linearities need be included in a first analysis. For example, cushion pressures of practical interest are usually low enough to make the lumped capacitance approximation of the compression process very accurate. Also, although numerical simulations by Hinchey [7] have shown that there may be large variations of fan pressure and fan volume flow associated with limit cycle oscillations, these oscillations can occur when the air source pressure is held constant [7]. Finally, in view of the uncertainty about the practical significance of the hysteresis phenomena, it seems appropriate to omit them here. Consequently attention is restricted to the two that seem universally characteristic of ACV's, the Bernoulli law for orifice flows, and shut-off.

## 3. AIR CUSHION MODEL AND EQUATIONS

The basic models are shown in Figures 1(a) and (b). A fan with a known static pressure–volume flow characteristic for gauge pressure $p_f$ as a function of volume flow $Q_f$ pumps air through an orifice of diameter $D_f$ into either a supply box having a volume $V_b$ or a circular supply duct of diameter $D_d$ and length $L_d$. The supply system in turn feeds a single cell plenum chamber through an orifice having diameter $D_c$. The fan, supply system, and cushion are free to move as a single rigid unit, so the system has one degree of freedom, the distance $x$ of a reference point on the vehicle above an inertial datum line. The cushion skirt is depicted as a slightly tapered truncated cone having a base diameter $D_p$ and height $L_p$. It is made of a very flexible but inextensible membrane, and the slight taper introduces a longitudinal tension into the membrane in order to keep it deployed. When it is moving, but with the skirt not contacting the ground, the hovergap $h$ is uniform around the periphery of the cone. The inertial datum is chosen such that $x = h$ for $x \geq 0$.

When $x \leq 0$, skirt–ground contact occurs, and the bottom part of the skirt is forced to collapse. Observations of this type of skirt in motion indicate that the typical skirt material is so thin and flexible that collapse occurs only in a very small region close to the ground-plane and that the deployed portion remains conical as shown in Figure 2.

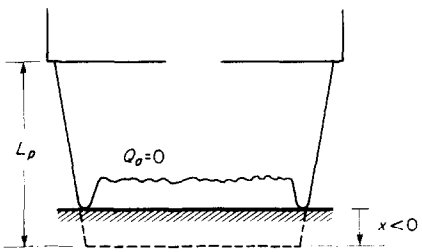


Figure 2. Assumed behaviour of skirt for $x < 0$.

Consequently, it is assumed that the vertical force generated by the cell may be calculated by assuming that the cell pressure is uniform and acts over the area defined by the intersection of the fully deployed cell and the ground plane. This assumption was made for the development of a theory for the static roll stiffness of a cushion system with these cells as the basic element, and it was found to be adequate [10]. The skirt material is also assumed to be so light that it adjusts quasi-statically to the motion of the cushion.

The equations governing the motion can be formulated as follows. First, Newton's law for the forces on the cushion system is

$$m\, \mathrm{d}^2x/\mathrm{d}t^2 = S_a(x)p_c - mg. \tag{1}$$

In equation (1), $m$ is the mass of the system, $t$ is time, $S_a(x)$ is the pressurized support or "foot-print" area, $p_c$ is the cushion gauge pressure and $g$ is the acceleration due to gravity. The foot-print area is a non-linear function of $x$; with $\Phi$ = skirt taper angle

$$S_a(x) = (\pi/4)(D_p - 2x \tan \Phi)^2 \text{ for } x < 0, \qquad S_a(x) = S_{a0} = (\pi/4)D_p^2 \text{ for } x \geq 0. \tag{2a, b}$$

Usually $x/D_p \ll 1$ so that equation (2a) is accurately approximated by

$$S_a(x) = S_{a0} - L_c x \tan \Phi, \tag{2c}$$

where $L_c$ is the length of the perimeter of the skirt bottom, which is $\pi D_p$ here. For the

model depicted in Figure 1, $\phi \ll 1$ so that $S_a$ is approximated accurately by $S_{a0}$ for values of $x$ of interest.

The second equation is the mass conservation statement for the cushion volume:

$$(\mathrm{d}/\mathrm{d}t)(\rho_c V_c) = \dot{m}_c - \dot{m}_a. \tag{3}$$

In equation (3), $\dot{m}_c$ is the mass flux between the supply system and cushion volume $V_c$ and $\dot{m}_a$ is the mass flux from cushion to atmosphere. The volume $V_c$ is a function of $x$, that is,

$$V_c = V_{c0} + S_{a0}x, \tag{4}$$

where $V_{c0}$ is the volume contained by the fully deployed skirt. As for the computation of $S_{a0}$, equation (4) applies only when $x/D_p \ll 1$. With the assumption that the cushion volume can be treated as a lumped pneumatic capacitance, equations (3) and (4) are replaced by

$$C_c\dot{p}_c + S_a\dot{x} = Q_c - Q_a, \tag{5}$$

where $Q$ is the volume flux of air, and

$$C_c = V_c/\rho_a a^2. \tag{6}$$

Here, $C_c$ is the pneumatic capacitance of the cushion volume and $a$ is the atmospheric sound speed.

Two cushion air supply systems are considered. One is a plenum supply box, which is modelled by a pneumatic capacitance:

$$C_b\dot{p}_b = Q_f - Q_c, \qquad C_b = V_b/\rho_a a^2. \tag{7}$$

The other is a moderately long duct, which is modelled by a lumped inertance [5, 6]:

$$(\rho_a L_d/A_d)\dot{Q}_d = p_{df} - p_{dc}. \tag{8}$$

The quantities $L_d$ and $A_d$ are the length and the cross-sectional area of the duct respectively, and $p_{df}$ and $p_{dc}$ are the pressures in the duct at the fan end and cushion end respectively. With equilibrium values denoted by a subscript $e$, the losses make $p_{dfe} < p_{fe}$ and $p_{dce} > p_{ce}$ since a stabilizing orifice is included at the cushion inlet.

The orifice flows and the cushion air escape process are assumed to be inviscid, incompressible and quasi-steady. Thus

$$Q_a = \pm C_m L_c h\sqrt{|(2p_c/\rho_a)|}. \tag{9}$$

This form of the equation allows for the possibility of flow reversal; $C_m$ is a discharge coefficient, here assumed to be 0·61. The flow from the supply system into the cushion is governed by

$$Q_c = \pm C_m A_c\sqrt{|2(p_i - p_c)/\rho_a|}, \tag{10}$$

where $A_c$ is the stabilizing orifice area, $i = b$ for the box case, and $i = dc$ for the duct case. For both cases it is assumed that a feed orifice separates the fan from the supply, in which case one has

$$Q_f = \pm C_m A_i\sqrt{|2(p_f - p_i)/\rho_a|}, \tag{11}$$

where $i = b$ for the box case and $i = df$ for the duct case.

Now modelling shut-off and flow reversal by the quasi-steady relationships (9)–(11) requires that the contribution of the unsteady inertia terms must be small compared to the convective inertia terms. For ACV processes which are small perturbations about a

non-zero mean flow this requirement is usually satisfied. If flow reversal occurs, then for at least part of the time, the unsteady inertia terms will be important or dominant. Indeed, around flow reversal, it could be argued that the correct model of the motion is that used to describe the processes in a Helmholtz orifice–cavity resonator [12, p. 186]. However, in an investigation of the frequency response characteristics of an air cushion suspension subject to heaving ground-board inputs, described in reference [13], the effect of orifice–cavity systems intended to act as dampers were evaluated. Good agreement between the results obtained from a non-linear theory—based essentially on the assumptions employed for the present analysis—and the experimental data for a wide range of frequencies, including the resonance peak for the system, strongly suggest that the Bernoulli model of the orifice flow is a useful approximation for most of the oscillatory cycle. Hence its use here is believed to be appropriate.

Two additional equations are required to form a closed system. The first is a linear fan law:

$$p_f = p_{f0} + C_s Q_f. \tag{12}$$

Here $p_{f0}$ is the fan supply pressure corresponding to zero $Q_f$, and $C_s$ is a given constant. The second is the relationship between $h$ and $x$, which is

$$h = x \text{ for } x > 0, \qquad h = 0 \text{ for } x < 0. \tag{13}$$

It is noted that, although the cushion geometry used here was chosen for its simplicity, it is easy to extend it to more complicated geometries. For many practical geometries, the footprint is not circular, and $\Phi$ is not small, but equation (2) with an appropriate calculation of $L_c$ describes these cases.

## 4. METHOD OF ANALYSIS

Numerical simulations [6, 7] have shown that the amplitudes of the oscillations in $x$ and $p_c$ are usually large compared with $x_e$ and $p_{ce}$. However, there are only a few methods available for the analysis of non-linear oscillations which do not involve the assumption that the amplitudes are small. One such technique is an extension of block diagram concepts developed for the treatment of linear automatic control systems. It is generally known as the describing function technique, and it has been successfully applied to a wide variety of problems, including such highly non-linear phenomena as relays, deadband and hysteresis [9].

In this technique the problem is formulated as a block diagram in which the linear and non-linear elements are identified. For example, consider the Van der Pol oscillator

$$\ddot{y} - \alpha(1 - \beta y^2)\dot{y} + y = \ddot{y} - \alpha(\mathrm{d}/\mathrm{d}t)(y - \beta y^3/3) + y = f(t). \tag{14}$$

For a limit cycle, the input function $f(t)$ is zero. Figure 3 is a canonical block diagram for this problem, and $s = \sigma + \mathrm{j}\omega$ is the Laplace variable. In the general case it is assumed

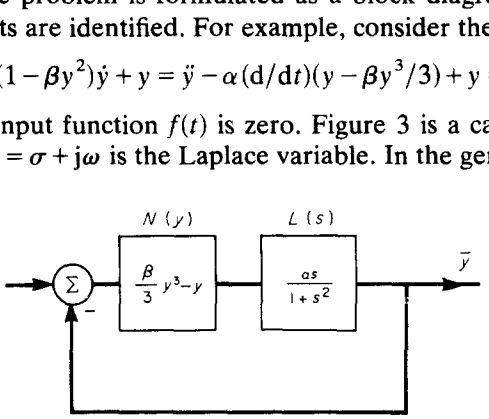


Figure 3. A canonical block diagram for the Van der Pol oscillator.

that the input to the non-linearity $N(y)$ can be approximated by $y \approx y_a = A_0 + A_1 \sin \psi$, with $\psi = \omega t + \phi$. The so-called dual input describing function (DIDF) is obtained by Fourier analysis of the output of $N(y) = Z(t)$ that would occur in response to the approximate input $y_a$, and retention of the constant or bias term and the first harmonic. That is, if $Z_a(t)$ is the sum of these two terms,

$$Z_a(t) \triangleq A_0\{N_B\} + A_1(\{n_p\} \sin \psi + \{n_q\} \cos \psi), \qquad N_A = n_p + jn_q. \tag{15}$$

Here $N_B(A_0, A_1, \omega)$ and $N_A(A_0, A_1, \omega)$ are defined as the describing functions. For steady state oscillations to exist, according to the DF approach, both the sinusoid and the bias must propagate unattenuated around the loop in Figure 3, which gives, respectively,

$$N_A(A_0, A_1, \omega)L(j\omega) = -1, \qquad A_0 N_B(A_0, A_1, \omega)L(j0) = -A_0. \tag{16, 17}$$

This gives three real equations for $A_0$, $A_1$ and $\omega$.

The success of the method depends on the assumption that second and higher order harmonics can be omitted at the input to the non-linearity. This does not mean that the second and higher harmonics generated at the output in response to $y_a = A_0 + A_1 \sin \psi$ must be small. For most practical systems, the linear parts of the system $L(j\omega)$ act as a low pass filter, and these harmonics are greatly attenuated. This is the so-called "filter" hypothesis. The analytical justification for the filter hypothesis given by Gelb and Vander Velde [9, p. 625] amounts to the requirement that

$$|L(jk\omega)| \ll |L(j\omega)| \text{ for } k = 2, 3, \ldots. \tag{18}$$

The method is generally considered to have two major limitations. The first is that considerable physical insight may be required to ascertain if the condition (18) is satisfied, and for anything but relatively simple systems this may be difficult to achieve. Alternatively, the method must be used to obtain an estimate of $\omega$ and then the condition (18) checked. If significant second harmonic content is present, then a "bias plus two-sinusoid" DF would have to be developed. The second limitation is that many non-linear problems are originally posed as differential equations, and it may be cumbersome or even impossible to formulate them in terms of block diagrams. Gelbe and Vander Velde [9, p. 83] distinguish between explicit and implicit non-linearities in this respect, and for the latter class suggest assuming a form for the output $Z_a(t)$ and solving for the input by the method of harmonic balance [14, p. 59].

It is suggested here that, when these difficulties occur—as is the case for the ACV problem—it may be useful to recognize that the DF approach is equivalent to the application of a Galerkin procedure to the system differential equations with an assumed solution of the form

$$y_a = A_0 + \sum_{k=1}^{N} (A_k \sin k\omega t + B_k \cos k\omega t). \tag{19}$$

This is a point that has apparently been largely ignored in the recent literature [15–19]. For example, Bergen and Franks [18] in developing a rigorous justification of the DF method have made only an oblique reference to the work by Cesari [19] on the application of the Galerkin method to the same class of problem. The equivalence may be demonstrated by working selected classes of problems. A demonstration for the Van der Pol oscillator is given in the Appendix. This demonstration also shows that, for limit cycle oscillations, a non-linear eigenvalue problem is obtained, because the solution must be valid for arbitrary phase.

Although formulation of a problem by a Galerkin procedure may be simpler in some cases, the difficulty about the possible significance of higher harmonics remains. Also,

to determine the stability of a limit cycle a special formulation along the lines described by Gelb and Vander Velde for the DF philosophy [9, p. 120] is required. As shown by Nayfeh and Mook [14, p. 130], a small amplitude analysis automatically gives information on both of these questions. However, for the present work, since the objective is to compare the results of the analysis with numerical simulations, the questions of higher harmonics and stability are addressed.

## 5. GALERKIN PROCEDURE APPLIED TO ACV PROBLEM: THE PLENUM BOX SUPPLY CASE

When there is neither flow reversal nor shut-off, and the air source has constant $p_f = p_{f0}$, the differential equations are

$$m\ddot{x} = S_a P_c - mg, \tag{20}$$

$$S_a\dot{x} + C_c\dot{p}_c = C_m A_c\sqrt{2(p_b - pc)/\rho} - C_m Lx\sqrt{2p_c/\rho}, \tag{21}$$

$$C_b\dot{p}_b = C_m A_f\sqrt{2(p_{f0} - p_b)/\rho} - C_m A_c\sqrt{2(p_b - p_c)/\rho}. \tag{22}$$

The Galerkin procedure is applied as described, e.g., in reference [20]. To obtain a first order solution one puts $\tau = \omega t$, and

$$x_a = x_0 + x_1 \sin\tau, \qquad p_{ca} = p_{c0} + p_{c1}\sin(\tau + \phi_{c1}), \qquad p_{ba} = p_{b0} + p_{b1}\sin(\tau + \phi_{b1}). \tag{23–25}$$

Note that the phase of $x$ is chosen to simplify manipulation; the phases of other variables are determined by the analysis relative to that of $x$. The residual for equation (20) is $\varepsilon_N$, where

$$\varepsilon_N = \omega^2 m x_1 \sin\tau + s_a[p_{c0} + p_{c1}\sin(\tau + \phi_{c1})] - mg \tag{26}$$

and the integrals $\int_0^{2\pi}\varepsilon_N d\tau = \int_0^{2\pi}\varepsilon_N \sin\tau\, d\tau = \int_0^{2\pi}\varepsilon_N \cos\tau\, d\tau = 0$ give, respectively,

$$S_a p_{c0} = mg, \qquad \omega^2 m x_1 + S_a p_{c1}\cos\phi_{c1} = 0, \qquad S_a p_{c1}\sin\phi_{c1} = 0, \tag{27–29}$$

from which one has

$$p_{c0} = mg/S_a = p_{ce}, \qquad \phi_{c1} = 180°, \qquad \omega^2 m x_1 - S_a p_{c1} = 0. \tag{30}$$

However, application of the procedure to the other equations is not so straightforward. The residual $\varepsilon_c$ for the cushion capacitance equation is

$$\varepsilon_c = \omega[S_a x_1 - C_c p_{c1}]\cos\tau + (2/\rho_a)^{1/2} C_m L_c[(x_0 + x_1\sin\tau)(p_{ce} - p_{c1}\sin\tau)^{1/2}]$$
$$-(2/\rho_a)^{1/2} C_m A_c[p_{b0} - p_{ce} + p_{b1}\sin(\tau + \phi_{b1}) + p_{c1}\sin\tau]^{1/2}. \tag{31}$$

The integral $\int_0^{2\pi}\varepsilon_c\, d\tau = 0$ becomes

$$L_c\left[x_0\int_0^{2\pi}(p_{ce} - p_{c1}\sin\tau)^{1/2}\, d\tau + x_1\int_0^{2\pi}\sin\tau(p_{ce} - p_{c1}\sin\tau)^{1/2}\, d\tau\right]$$
$$-A_c\left[\int_0^{2\pi}(p_{b0} - p_{ce} + p_{b1}\sin(\tau + \phi_{b1}) + p_{c1}\sin\tau)^{1/2}\, d\tau\right] = 0. \tag{32}$$

Most of the integrals in equation (32) and others that are formed in applying the Galerkin procedure are elliptic. Many of these forms have been tabulated [21]. However, the standard forms required depend on the relative magnitudes of the unknown coefficients, which are parameters in the integrals.

The task of reducing the integrals to standard form is particularly onerous when shut-off and flow reversal are included. Consequently, numerical methods were used. Equation (32) and its companions comprise a set of non-linear algebraic equations $f_i(\mathbf{x}) = 0$, $i = 1, 2, \ldots, N$, for the vector of unknowns $\mathbf{x} = (x_0, x_1, p_{c1}, \ldots \phi_{b1})^T$. Given $\mathbf{x}^{(k)}$, the $k$th approximation to $\mathbf{x}$, the integrations in equations such as equation (32) were computed by using Simpson's rule (100 points). This gave $f_i^{(k)}(\mathbf{x})$. The Newton–Raphson technique was then applied to generate $\mathbf{x}^{(k+1)}$:

$$\mathbf{x}^{(k+1)} = \mathbf{x}^{(k)} - \lambda (\partial f_i / \partial \mathbf{x})^{-1} \mathbf{f}_i[\mathbf{x}^{(k)}]. \tag{33}$$

The square matrix of derivatives $\partial f_i / \partial \mathbf{x}$ at each $\mathbf{x}^{(k)}$ was determined by a finite difference procedure, and the factor $\lambda < 1$ was included to ensure convergence. It is noted that, for an inappropriate initial estimate of the unknowns, the process would either diverge or converge to the unstable trivial solution $x_1 = 0$, $p_{c1} = 0$, $p_{b1} = 0$.

## 6. TYPICAL RESULTS

### 6.1. PLENUM BOX SUPPLY MODEL

Numerical results have been obtained for a plenum box supply model with $D_p = 1{\cdot}83$ m and height $L_p = 0{\cdot}914$ m. The box volume $V_b = 1{\cdot}415\ \text{m}^3$, and the feed areas $A_c = A_f = 0{\cdot}073\ \text{m}^3$. The fan slope coefficient $C_s$ is set equal to zero. This geometry is representative of that used on a multicell system developed for a towed raft application.

The linear heave stability boundary for this system in terms of cushion pressure $p_{ce}$ and hovergap $h_e$ is obtained from equations (1) to (13) in the usual way [4–7]. The results are given in Figure 4; the hatched side of the curve indicates the unstable region. Points $a$, $b$ and $c$, corresponding to $h_e = 4{\cdot}58$ mm, are examined for limit cycle behaviour. Typical first order Galerkin results are given in Table 1. For these the initial estimates given in Table 2 were used. The results indicate that a limit cycle does exist in the unstable region close to the boundary and that, as might be expected, the amplitude of the oscillation increases with increase in distance from the boundary.

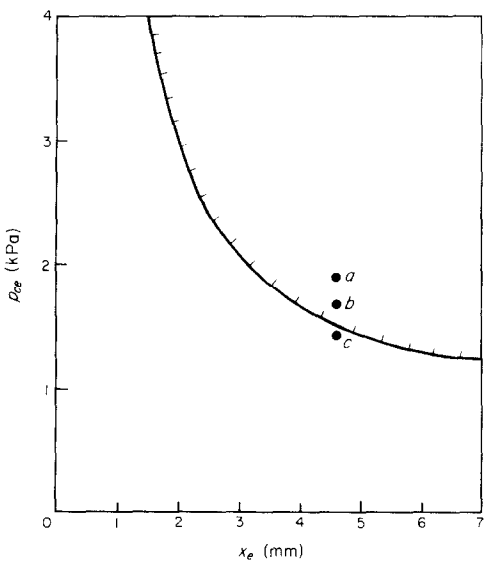


Figure 4. Linear heave stability boundary for plenum box supply system.

TABLE 1

*Typical Galerkin results for plenum box supply model with first order harmonics only; hovergap $h_e = 4{\cdot}58$ mm; lengths in mm, pressures in kPa*

| Operating point | Variable | $\omega$ | Coefficients in expansion | | |
|---|---|---|---|---|---|
| | | | | First harmonic | |
| | | | Constant | Amplitude | Phase |
| $a$ | $x$ | | 4·12 | 4·17 | 0 |
| $p_{ce} = 1{\cdot}914$ | $p_c$ | 26·04 | 1·9147 | 0·552 | +180° |
| | $p_b$ | | 2·1613 | 0·275 | +177·0° |
| $b$ | $x$ | | 4·38 | 3·21 | 0 |
| $p_{ce} = 1{\cdot}675$ | $p_c$ | 27·84 | 1·6754 | 0·425 | +180° |
| | $p_b$ | | 1·8928 | 0·212 | +176·5° |
| $c$ | $x$ | | 4·57 | 0 | |
| $p_{ce} = 1{\cdot}436$ | $p_c$ | 30·07 | 1·4360 | 0 | |
| | $p_b$ | | 1·6221 | 0 | |

TABLE 2

*Initial estimates for iteration: plenum box supply case*

| Variable | Coefficients in expansion | | | | |
|---|---|---|---|---|---|
| | | First harmonic | | Second harmonic | |
| | Constant | Amplitude | Phase | Amplitude | Phase |
| $x$ | $x_e$ | $\dfrac{S_a(p_f - p_{ce})}{m\omega_{\text{lin}}^2}$ | 0 | 0 | 0 |
| $p_c$ | $p_{ce}$ | $p_f - p_{ce}$ | 180° | 0 | 0 |
| $p_b$ | $p_{be}$ | $p_f - p_{be}$ | 180° | 0 | 0 |
| $\omega$ | Linear eigenvalue analysis | | | | |

Numerical results obtained from a Runge–Kutta integration of the governing non-linear equations are shown in Figure 5. Fourier decompositions of the signals are given in Table 3. On comparing Tables 1 and 3, one can see that for point $b$ the agreement is quite good, whereas for point $a$ it is not. Table 4 gives Galerkin results for point $a$ obtained with second order harmonics retained. On comparing these results with those in Table 3, one can see that the agreement with the harmonics included is much improved. Figure 5 suggests that the higher harmonics are associated primarily with shut-off.

### 6.2. DUCT SUPPLY MODEL

Numerical results have also been obtained for a duct supply model with cushion and feed areas having the same dimensions as in the plenum box supply model. The duct has the same volume as the box; it is 6·1 m long and 0·544 m in diameter. This is typical of the multicell mentioned previously as modified for overwater operation. As for the previous results $C_s$ is set equal to zero.

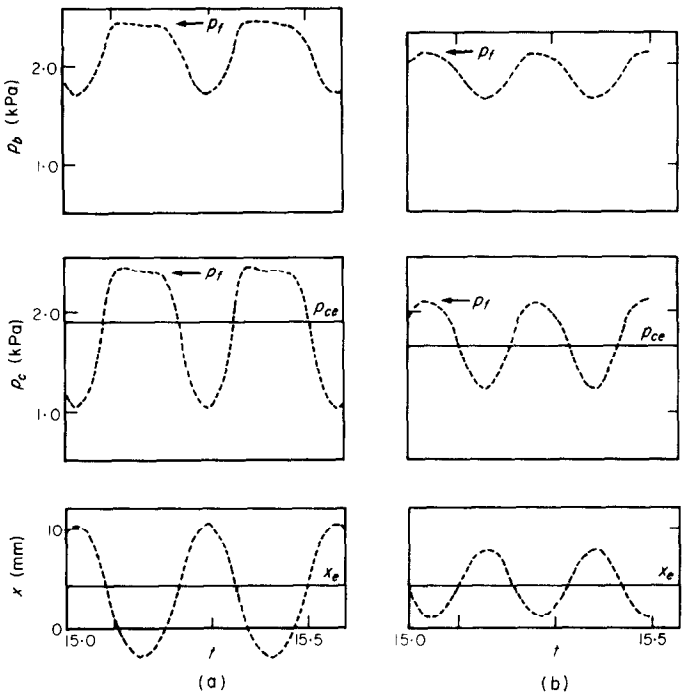


Figure 5. Runge–Kutta numerical integration results for plenum box supply system.

TABLE 3

*Fourier decomposition of numerical simulation for plenum box supply model; hovergap* $h_e = 4{\cdot}58$ *mm*

| Operating point | Variable | Frequency $\omega$ | Coefficients in expansion: Constant | First harmonic: Amplitude | First harmonic: Phase | Second harmonic: Amplitude | Second harmonic: Phase |
|---|---|---|---|---|---|---|---|
| | $x$ | | 3·26 | 6·65 | 0 | 0·46 | +106° |
| $a$ | $p_c$ | 23·3 | 1·916 | 0·715 | 180° | 0·211 | −94° |
| | $p_b$ | | 2·162 | 0·354 | +177° | 0·107 | −105° |
| | $x$ | | 4·39 | 3·37 | 0 | 0·05 | +79° |
| $b$ | $p_c$ | 27·9 | 1·675 | 0·451 | 180° | 0·03 | −116° |
| | $p_b$ | | 1·893 | 0·224 | +176° | 0·0170 | −138° |

TABLE 4

*Galerkin results for point "a" with second harmonics included*

| Variable | Frequency $\omega$ | Constant | First harmonic: Amplitude | First harmonic: Phase | Second harmonic: Amplitude | Second harmonic: Phase |
|---|---|---|---|---|---|---|
| $x$ | | 3·21 | 7·06 | 0 | 0·600 | +79° |
| $p_c$ | 23·16 | 1·915 | 0·739 | 180° | 0·251 | −101° |
| $p_b$ | | 2·164 | 0·368 | +176° | 0·135 | −109° |

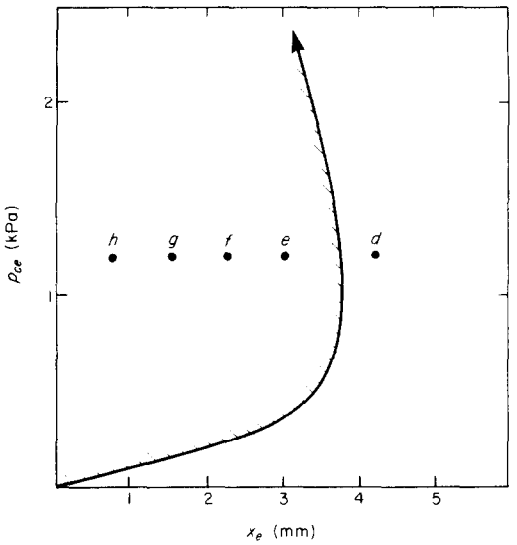


Figure 6. Linear heave stability boundary for duct supply system.

The linear heave stability boundary for this system is shown in Figure 6. An important point to note in Figure 6 is that, whereas the plenum box supply model is very stable at low flows or hovergaps, the duct supply model is unstable. In references [6, 7] it is shown that this instability is a Helmholtz resonator effect associated with the inertia of the duct air and the cushion capacitance. Here, points *d* to *h* have been examined for limit cycle behaviour. Typical first order Galerkin results are given in Table 5. For these, the initial estimates given in Table 6 were used. The amplitude of the signals for $x$ in

TABLE 5

*Typical Galerkin results for duct supply model with first order harmonics only*; $p_{ce} = 1{\cdot}197$ *kPa*

| Operating point | Variable | Frequency $\omega$ | Coefficients in expansion | | |
|---|---|---|---|---|---|
| | | | Constant | First harmonic | |
| | | | | Amplitude | Phase |
| *e* | $x$ | | 2·77 | 3·32 | 0 |
| $h_e = 3{\cdot}05$ | $p_c$ | 54·0 | 1·197 | 1·178 | 180° |
| | $Q_d$ | | 0·2595 | 0·6797 | −75·9 |
| *f* | $x$ | | 1·44 | 3·29 | 0 |
| $h_e = 2{\cdot}29$ | $p_c$ | 54·3 | 1·197 | 1·183 | 180° |
| | $Q_d$ | | 0·1480 | 0·6810 | −77·5 |
| *g* | $x$ | | −0·05 | 2·86 | 0 |
| $h_e = 1{\cdot}52$ | $p_c$ | 54·5 | 1·197 | 1·039 | 180° |
| | $Q_d$ | | 0·0750 | 0·6014 | −79·5 |
| *h* | $x$ | | −0·81 | 1·90 | 0 |
| $h_e = 0{\cdot}76$ | $p_c$ | 54·9 | 1·197 | 0·694 | 180° |
| | $Q_d$ | | 0·0279 | 0·4048 | −83·1 |

TABLE 6

*Initial estimates for iteration: duct supply case*

| | Coefficients in expansion | | |
|---|---|---|---|
| | | First harmonic | |
| Variable | Constant | Amplitude | Phase |
| $x$ | $x_e$ | $\frac{S_a p_{ce}}{m\omega_{\text{lin}}^2}$ | 0 |
| $p_c$ | $p_{ce}$ | $p_{ce}$ | 180 |
| $Q_d$ | $Q_{de}$ | $\frac{A_d}{L_d \rho}\frac{p_{ce}}{\omega}$ | −90 |
| $\omega$ | Linear eigenvalue analysis | | |

Table 5 is plotted in Figure 7. This plot shows how the amplitude first increases rapidly with distance from the stability boundary and then decreases as $h_e$ approaches zero.

Numerical results for $x$ obtained from a Runge–Kutta integration of the governing equations are shown in Figure 8. Fourier decompositions of these signals together with those for $p_c$ and $Q_d$ for points $e$ and $g$ are given in Table 7. Comparison with the Galerkin results shows that the agreement is reasonable.

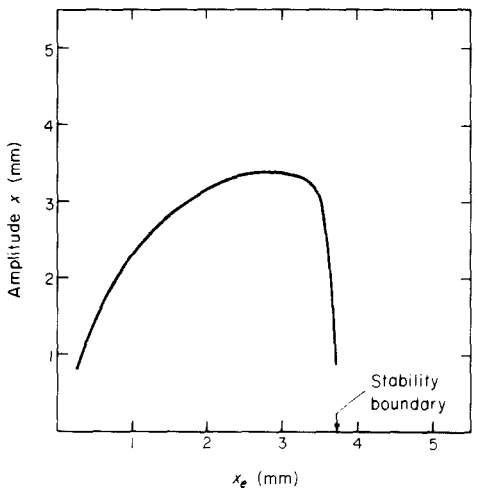


Figure 7. Amplitude of limit cycle for duct supply system.

## 6.3. LIMIT CYCLE SUPPRESSION

In a series of papers published in the late 1950's and early 1960's, Oldenburger and his colleagues [22–25] demonstrated experimentally and confirmed theoretically that a high frequency signal at the input to the non-linearity of a limit cycling control system could quench or suppress the limit cycle. Using describing function theory, they showed how this "dither" signal modified the input–output characteristics of the non-linearity.

It is shown here that a similar procedure can be used to suppress ACV limit cycle oscillations. For the present problem, a high frequency pressure signal is introduced by

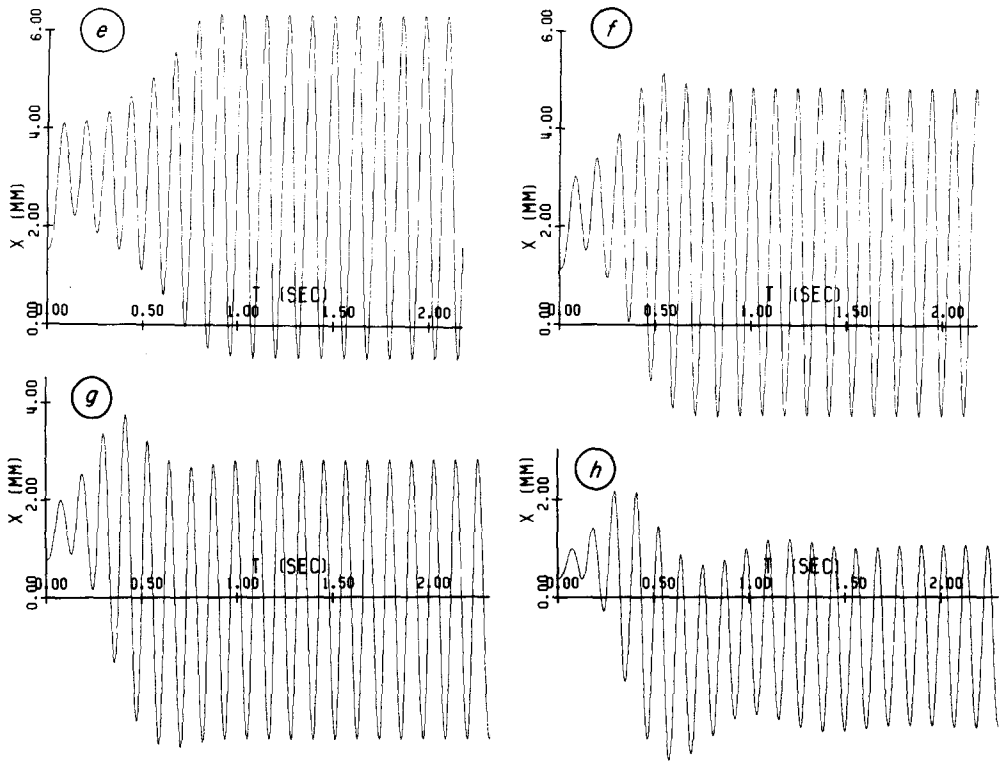


Figure 8. Runge–Kutta results for duct supply system.

TABLE 7

*Fourier decomposition of numerical simulation for duct supply model*; $p_{ce} = 1{\cdot}197$ *kPa*

| Operating point | Variable | Frequency $\omega$ | Coefficients in expansion | | | | |
|---|---|---|---|---|---|---|---|
| | | | | First harmonic | | Second harmonic | |
| | | | Constant | Amplitude | Phase | Amplitude | Phase |
| $e$ | $x$ | | 2·84 | 3·51 | 0 | 0·1275 | −165 |
| $h_e = 3{\cdot}05$ | $p_c$ | 52·8 | 1·197 | 1·190 | 180 | 0·153 | 16 |
| | $Q_d$ | | 0·2663 | 0·7023 | −75·8 | 0·0586 | 91·9 |
| $g$ | $x$ | | −0·07 | 2·85 | 0·0 | 0·0036 | 47·8 |
| $h_e = 1{\cdot}52$ | $p_c$ | 54·6 | 1·197 | 1·030 | 180 | 0·013 | −160 |
| | $Q_d$ | | 0·0747 | 0·6003 | −79·7 | 0·0070 | −4·6 |

adding to the mass conservation equation for the cushion a term which gives a periodic volume variation: that is,

$$C_c \dot{p}_c = (Q_c - Q_a) - S_a \dot{x} + (\mathrm{d}/\mathrm{d}t)(\Delta V_0), \qquad \Delta V_0 = C_d \sin(\omega_d t). \tag{34, 35}$$

Following Oldenburger, one can set $\omega_d = 10\omega$. This volume variation, which may be obtained by using a piston, induces a high frequency pressure variation which serves as an extra input into the non-linearities.

TABLE 8

*Galerkin limit cycle quenching results for plenum box supply system; hovergap* $h_e = 4{\cdot}58$ *mm*

| Operating point | Variable | Coefficients in expansion | | | | |
|---|---|---|---|---|---|---|
| | | | First harmonic | | Dither content | |
| | | Constant | Amplitude | Phase | Amplitude | Phase |
| *a* | $x$ | 3·51 | 0·0 | | 0·045 | 20 |
| | $p_c$ | 1·9147 | 0·0 | | 0·5940 | −160 |
| | $p_b$ | 2·1881 | 0·0 | | 0·2591 | 173·0 |
| *b* | $x$ | 3·26 | 0·0 | | 0·045 | 20 |
| | $p_c$ | 1·6754 | 0·0 | | 0·5966 | −160 |
| | $p_b$ | 1·9161 | 0·0 | | 0·2548 | 174 |

Typical Galerkin results for the plenum box supply system with $C_d = 0{\cdot}012$, which, for the present geometry, gives a cushion volume variation from equilibrium of only 0·5% of the basic cushion volume, are given in Table 8, where the subscript $d$ indicates a component associated with the dither signal. These results show that the limit cycles at *a* and *b* have been effectively quenched. They are in close agreement with results obtained from a Runge–Kutta numerical integration. It is interesting to note that the volume variation creates bias values of $p_c$ and $x$, namely, $p_{c0}$ and $x_0$, which when plotted in Figure 4 lie in or close to the stable region. The quenching effect is probably associated with this shift. With $C_d = 0{\cdot}006$, the limit cycles are not quenched. However, they are reduced in amplitude and again this is believed to be associated with a shift in bias values. A typical result is given in Table 9.

TABLE 9

*Galerkin limit cycle suppression results for plenum box supply system; hovergap* $h_e = 4{\cdot}58$ *mm, point "a"*

| Variable | Coefficients in expansion | | | | |
|---|---|---|---|---|---|
| | | First harmonic | | Dither content | |
| | Constant | Amplitude | Phase | Amplitude | Phase |
| $x$ | 4·05 | 3·51 | 0 | 0·022 | 20 |
| $p_c$ | 1·9147 | 0·4660 | 180 | 0·2958 | −160 |
| $p_b$ | 2·1687 | 0·2338 | 176·6 | 0·1286 | 175 |

## 7. CONCLUSIONS

Application of a Galerkin/describing function technique to the equation describing the motion of two simple air cushion systems confirms inferences made from detailed numerical simulations, namely that the motion near linear stability boundaries is usually a limit cycle. The limit cycle is associated with the non-linearities that seem to be universally characteristic of an air cushion: the Bernoulli law governing the quasi-steady air flow escape process from the cushion coupled to the varying hovergap, and the

phenomenon of shut-off. Even for operationg points which are close to stability boundaries, the oscillations in gap $h$ and cushion pressure $p_c$ may be large compared to their respective equilibrium values. Comparison of the results of a Galerkin/describing function analysis with those obtained from Fourier analysis of detailed numerical simulations show that, when shut-off occurs, significant second order harmonics may be present.

The approximate technique used in the present work is well suited to the analysis of large non-linearities, but it has two associated difficulties. One is the computational burden, and the other is that, at a given level of approximation, no indication is given as to the significance of omitted higher order harmonics. Also, a complete investigation should, ideally, include a stability analysis similar to that described by Gelb and Vander Velde [9].

Finally it is shown that an equivalent of the "artificial dither" technique used in the describing function literature for suppression of limit cycles may also be used to suppress air cushion oscillations. This is achieved by introducing a very small high frequency oscillation to the cushion volume. Its practical implementation seems to be straightforward. However, use of a quasi-steady orifice flow law is questionable because of the high "dither" frequencies involved. Thus, the idea needs to be confirmed experimentally.

## REFERENCES

1. H. S. FOWLER 1976 *National Research Council of Canada, Associate Committee on Air Cushion Technology, Technical Report* 5/76. Caspar ACV Research Project Report No. 4. The multicell skirt, a summary.
2. H. S. FOWLER 1979 *Private Communication.* National Research Council of Canada.
3. P. A. SULLIVAN, G. M. GREEN and P. V. HARTMANN 1979 *Canadian Symposium on Air Cushion Technology, Montreal.* Pitch and roll stiffness characteristics of a segmented skirt cushion.
4. W. A. RIBICH and H. H. RICHARDSON 1967 *Massachusetts Institute of Technology, Report DSR* 76110-3. Dynamic analysis of heave motion for a transport vehicle fluid suspension.
5. L. M. SWEET, H. H. RICHARDSON and D. N. WORMLEY 1975 *American Society of Mechanical Engineers, Paper No.* 75-*WA*/*AUT*-23. Plenum air cushions/compressor–duct dynamic interactions.
6. M. J. HINCHEY and P. A. SULLIVAN 1978 *Journal of Sound and Vibration,* **60**, 87–99. Duct effects on the heave stability of plenum air cushions.
7. M. J. HINCHEY 1979 *Ph.D. Thesis, University of Toronto.* Heave instabilities of amphibious air cushion suspension systems.
8. J. D. LEATHERWOOD 1971 *NASA TN D* 6257. Analog analysis of the heave response and control of a plenum type air cushion vehicle.
9. A. GELB and W. E. VANDER VELDE 1968 *Multiple Input Describing Functions and Nonlinear System Design.* New York: McGraw-Hill.
10. P. A. SULLIVAN, M. J. HINCHEY and R. G. DELANEY 1978 *Journal of Terramechanics* **15**, 15–49. Static roll stiffness characteristics of two multicell type air cushion systems.
11. P. A. SULLIVAN, M. J. HINCHEY, I. MURRA and G. J. PARRAVANO 1979 *University of Toronto, Institute for Aerospace Studies, Report No.* 238. Research on the stability of air cushion systems.
12. L. E. KINSLER and A. R. FREY 1962 *Fundamentals of Acoustics.* New York: John Wiley & Sons.
13. G. J. PARRAVANO and P. A. SULLIVAN 1977 *Transport Canada, Research and Development Centre, Contract Report D*-500-210. A theoretical and experimental investigation of a hinged lip tracked air cushion vehicle suspension system.
14. A. H. NAYFEH and D. T. MOOK 1980 *Nonlinear Oscillations.* New York: Wiley–Interscience.
15. K. KLOTTER 1956 *Polytechnic Institute of Brooklyn, New York, Proceedings of the Symposium on Nonlinear Circuit Analysis.* An extension of the conventional concept of the describing function.
16. K. KLOTTER 1957 *Transactions of the American Society of Mechanical Engineers* **79**, 509–512. How to obtain describing functions for nonlinear feedback systems.

17. P. JOHANSEN 1970 *Ph.D. Thesis, Purdue University*. A numerical formulation of Galerkin's method and its application to nonlinear engineering problems.
18. A. R. BERGEN and R. L. FRANKS 1971 *SIAM Journal of Control* **9**, 568–589. A justification of the describing function method.
19. L. CESARI 1962 *Contributions to Differential Equations: Volume* 1. New York: Wiley–Interscience. Functional analysis and periodic solutions of nonlinear differential equations.
20. B. A. FINLAYSON 1972 *The Method of Weighted Residuals and Variational Principles*. New York: Academic Press, first edition.
21. I. S. GRADSHTEYN and I. M. RYZHIK 1965 *Tables of Integrals, Series and Products*. New York: Academic Press, fourth edition.
22. R. OLDENBURGER 1957 *Transactions of the American Society of Mechanical Engineers* **79**, 1869–1872. Signal stabilization of a control system.
23. R. OLDENBURGER and C. C. LIU 1959 *Transactions of the American Institute of Electrical Engineers* **78**, 96–100. Signal stabilization of a control system.
24. R. OLDENBURGER and T. NAKADA 1961 *Institute of Radio Engineers Transactions on Automatic Control* **AC6**, 319–325. Signal stabilization of self oscillating systems.
25. R. OLDENBURGER and R. C. BOYER 1962 *Journal of Basic Engineering* **84**, 559–570. Effects of extra sinusoidal inputs to nonlinear systems.

## APPENDIX

For the non-linearity in Figure 3, from reference [9, p. 545]

$$N_B = 1-(\beta/3)(\tfrac{3}{2}A_1^2+A_0^2), \qquad N_A = n_p = 1-(\beta/3)(\tfrac{3}{4}A_1^2+3A_0^2). \tag{A1}$$

The two equivalent circuit conditions (16) and (17) give, respectively,

$$[1-(\beta/3)(\tfrac{3}{4}A_1^2+3A_0^2)](j\omega) = 1-\omega^2, \qquad A_0[1-(\beta/3)(\tfrac{3}{2}A_1^2+A_0^2)] = -A_0. \tag{A2, A3}$$

The only consistent solution of these equations is $A_0 = 0$, $\omega = 1$ and $A_1 = 2/\sqrt{\beta}$.

To obtain a first order approximation by a Galerkin procedure, one can try

$$y_a \approx A_0 + A_1 \sin \omega t + B_1 \cos \omega t. \tag{A4}$$

This procedure yields

$$\int_0^{2\pi/\omega} e\,dt = 0: A_0 = 0, \tag{A5}$$

$$\int_0^{2\pi/\omega} e \sin \omega t\, dt = 0: (1-\omega^2)A_1 + \alpha\omega B_1 - \tfrac{1}{4}\alpha\beta\omega B_1(A_1^2+B_1^2) = 0, \tag{A6}$$

$$\int_0^{2\pi/\omega} e \cos \omega t\, dt = 0: (1-\omega^2)B_1 - \alpha\omega A_1 + \tfrac{1}{4}\alpha\beta\omega A_1(A_1^2+B_1^2) = 0. \tag{A7}$$

Equations (A6) and (A7) can be manipulated to give

$$A_1^2 + B_1^2 = 4/\beta, \qquad (1-\omega^2)A_1 = (1-\omega^2)B_1 = 0. \tag{A8, A9}$$

It follows that non-zero solutions exist only if $\omega = 1$, in which case equation (A8) specifies only the amplitude of the oscillation and not the phase. This demonstrates the eigenvalue character of limit cycle problems. The result is identical to that obtained by the describing function method.